

## Polarization of Neutrons from the $C^{13}(p,n_0)N^{13}$ and $N^{15}(p,n_0)O^{15}$ Reactions\*†

B. D. WALKER, C. WONG, J. D. ANDERSON, J. W. McCLURE, AND R. W. BAUER‡  
Lawrence Radiation Laboratory, University of California, Livermore, California

(Received 31 July 1964)

The polarization of neutrons from the  $C^{13}(p,n_0)N^{13}$  and  $N^{15}(p,n_0)O^{15}$  reactions has been measured for proton energies in the region between 6.9 and 12.3 MeV and neutron-emission angles between 0 and 90°. The neutrons were detected using the Livermore time-of-flight facility incorporating pulse-shape discrimination to reduce the time-independent background. The "left" and "right" measurements were obtained by employing a solenoid for spin precession. Liquid helium was utilized as an analyzer. Large polarizations (50 to 70%) were measured for both reactions at several energies and angles. Corrections for multiple scattering in the analyzer have been made. The measurements are compared with the polarization predictions of the quasielastic model of the  $(p,n)$  process.

### INTRODUCTION

THE angular distribution of the neutrons from the  $C^{13}(p,n_0)N^{13}$  and  $N^{15}(p,n_0)O^{15}$  reactions has been measured by Wong *et al.*<sup>1</sup> for proton bombarding energies between 5 and 13 MeV. These studies were undertaken to investigate the suggestion of Bloom, Glendenning, and Moszkowski<sup>2</sup> that one may be able to deduce the effective neutron-proton interaction inside the nucleus from measurements of the ground state  $(p,n)$  reaction on mirror nuclei. It was further suggested that the above reactions are "twin" reactions; that is,<sup>2</sup> the interaction could be considered as taking place between the incoming (outgoing) particle and a  $p_{1/2}$  nucleon or nucleon hole in the field of a doubly closed shell nuclear core. The measurements of Wong *et al.*, tended to corroborate this direct reaction concept in that the changes in the angular distributions as the proton bombarding energy is increased are quite gradual. The similarity of the two sets of angular distributions, particularly at the higher energies, was also considered as confirming the twin reaction hypothesis. In order to provide a more sensitive test of the twin reaction concept, the angular (0–90°) and proton energy (7–12 MeV) dependences of the neutron polarizations for the two reactions  $C^{13}(p,n_0)N^{13}$  and  $N^{15}(p,n_0)O^{15}$  were measured.

Additionally, the measured polarizations are compared with quantitative polarization predictions obtained in the quasielastic interpretation of the  $(p,n)$  process. It has recently been pointed out by Lane<sup>3</sup> that the optical model potential should include a term proportional to  $\mathbf{t} \cdot \mathbf{T}$ , where  $\mathbf{t}$  is the isospin of the incident

nucleon and  $\mathbf{T}$  is the isospin of the target nucleus. In addition to reproducing the proton potential anomaly,<sup>4,5</sup> this isospin term can induce a  $(p,n)$  reaction in which the target nucleus is converted into its corresponding isobaric state. Specifically this term can induce the  $(p,n_0)$  transitions of interest here since the ground states of  $N^{13}$  and  $O^{15}$  are the corresponding isobaric states of  $C^{13}$  and  $N^{15}$ . Quasielastic  $(p,n)$  reactions in nonmirror medium- $A$  nuclei have been observed by Anderson *et al.*,<sup>6,7</sup> and Batty *et al.*<sup>8</sup>

Hansen and Stelts<sup>9</sup> have reported the angular distribution of the  $N^{15}(p,n_0)O^{15}$  reaction along with the predictions obtained by treating the isospin potential as a perturbation in distorted wave Born approximation (DWBA).<sup>10</sup> These calculations which included the effects of the Coulomb field on the incident wave and the fact that the neutron energy differs from the proton energy by the Coulomb displacement energy in the distorting potentials gave fair agreement with experiment for proton bombarding energies between 5 and 12 MeV.

### EXPERIMENTAL METHOD

Figure 1 is a schematic representation of the experimental geometry. The proton beam from the Livermore 90-in. variable energy cyclotron was incident on a 1-in.-diam by 1-in.-long gas target filled to 2 atm of  $CO_2$  (58%  $C^{13}$ ) or  $N_2$  (90%  $N^{15}$ ). Instead of performing the conventional left-right scattering measurements for determining the neutron polarizations, the neutron spin precession method<sup>11</sup> was employed. The neutrons

\* This work was performed under the auspices of the U. S. Atomic Energy Commission.

† A preliminary account of this work was presented at the American Physical Society, 1964, Washington, D. C. Meeting. Bull. Am. Phys. Soc. **9**, 444 (1964).

‡ Present address: Massachusetts Institute of Technology, Cambridge, Massachusetts.

<sup>1</sup> C. Wong, J. D. Anderson, S. D. Bloom, J. W. McClure, and B. D. Walker, Phys. Rev. **123**, 598 (1961).

<sup>2</sup> S. D. Bloom, N. R. Glendenning, and S. A. Moszkowski, Phys. Rev. Letters **3**, 98 (1959).

<sup>3</sup> A. M. Lane, Nucl. Phys. **35**, 676 (1962).

<sup>4</sup> A. E. Green and P. C. Sood, Phys. Rev. **111**, 1147 (1958).

<sup>5</sup> P. C. Sood, Nucl. Phys. **37**, 627 (1962).

<sup>6</sup> J. D. Anderson and C. Wong, Phys. Rev. Letters **7**, 250 (1961).

<sup>7</sup> J. D. Anderson, C. Wong, J. W. McClure, and B. D. Walker, Phys. Rev. **136**, B118 (1964).

<sup>8</sup> C. J. Batty, G. H. Stafford, and R. S. Gilmore, Phys. Letters **6**, 292 (1963).

<sup>9</sup> L. F. Hansen and M. L. Stelts, Phys. Rev. **132**, 1123 (1963).

<sup>10</sup> R. M. Drisko, R. H. Bassel, and G. R. Satchler, Phys. Letters **2**, 318 (1962).

<sup>11</sup> P. Hillman, G. H. Stafford, and C. Whitehead, Nuovo Cimento **4**, 67 (1956).

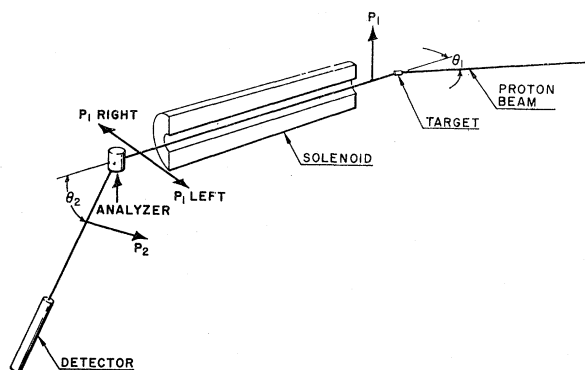


FIG. 1. Experimental geometry.

emerging at a reaction angle  $\theta_1$  with polarization<sup>12</sup>  $\mathbf{P}_1$  were collimated through a 40-in.-long solenoid magnet (3 in. i.d., 11 in. o.d.) and scattered by a liquid helium analyzer into the detector positioned about 12 in. from the analyzer and at a scattering angle  $\theta_2$ . ( $\theta_2$  was constant throughout the experiment at the lab angle of  $60^\circ$ .) The solenoid field causes a precession of the neutron polarization vector  $\mathbf{P}_1$  as the neutrons move through the field. By defining the scattering plane perpendicular to the reaction plane, the magnetic field need only be adjusted to precess  $\mathbf{P}_1$  through an angle

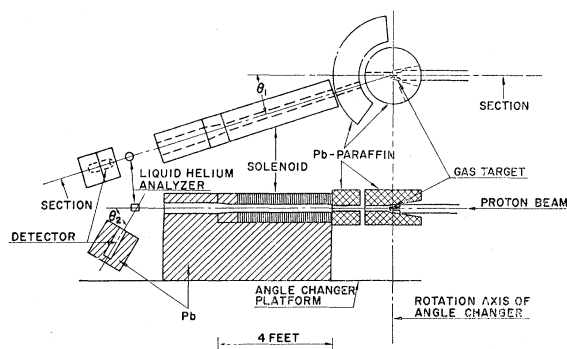


FIG. 2. Shielding geometry.

of  $\pi/2$ . For this geometry the polarization product (asymmetry) is given by

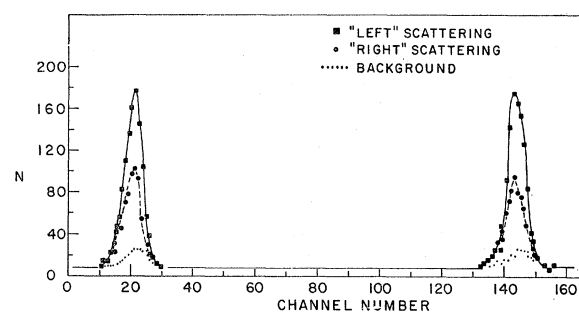
$$P_1 P_2 = \frac{N(+\pi/2) - N(-\pi/2)}{N(+\pi/2) + N(-\pi/2)}, \quad (1)$$

where  $N(\pm\pi/2)$  is the net number of helium scattered neutrons detected for  $\pm\pi/2$  precession and  $P_2$  is the analyzing power of helium.  $P_2$  is a function of the incident neutron energy as well as the scattering angle  $\theta_2$ . A knowledge of the direction of precession is essential for arriving at the correct sign for  $P_1$ . This direction

<sup>12</sup> The sense of the polarization vectors  $\mathbf{P}_1$  and  $\mathbf{P}_2$  is chosen in accordance with the Basel convention *Helv. Phys. Acta Suppl.* 6, 436 (1961), i.e.,  $\mathbf{P} = P(\mathbf{k}_i \times \mathbf{k}_f) / (|\mathbf{k}_i \times \mathbf{k}_f|)$ , where  $\mathbf{k}_i$  and  $\mathbf{k}_f$  are the initial and final propagation vectors, respectively.

was ascertained by determining the field direction and noting that the precession direction is given by  $\mathbf{B} \times \mathbf{P}_1$ , where  $\mathbf{B}$  is the magnetic field.

The liquid helium was contained in a thin-walled (0.005-in. stainless-steel) cylinder, 3 in. in diameter by 3 in. long with axis perpendicular to the reaction plane. The time-of-flight electronics with proton-electron pulse shape discrimination was similar to that of Ref. 1 with the exception that differential bias rather than integral bias was used to enhance the signal-to-background ratio of the helium-scattered neutrons. A detailed discussion of the liquid helium cryostat and electronics as well as other apparatus employed in this work may be found elsewhere.<sup>13</sup>

FIG. 3.  $C^{13} + p$  "left" and "right" helium-scattered neutron time spectrums ( $E_p = 6.9$  MeV,  $\theta_1 = 40^\circ$ ).

Considerable lead shielding placed beneath and at the exit of the solenoid (see Fig. 2) effectively attenuated the direct neutron flux. Approximately 12 in. of lead-paraffin completely enclosing the gas target assembly further reduced the time-independent background which arises principally from neutron capture gamma radiation at the walls of the experimental area. The weight of the solenoid and the required shielding was 5 tons with a center of gravity about 70 in. from the gas target. In order to measure the  $(p, n_0)$  polarization as a

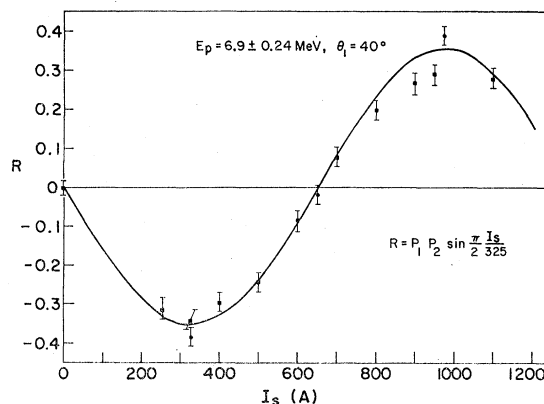


FIG. 4. Solenoid calibration curve.

<sup>13</sup> B. D. Walker, Ph.D. thesis, Lawrence Radiation Laboratory (Livermore) Report UCRL-7676 (1964).

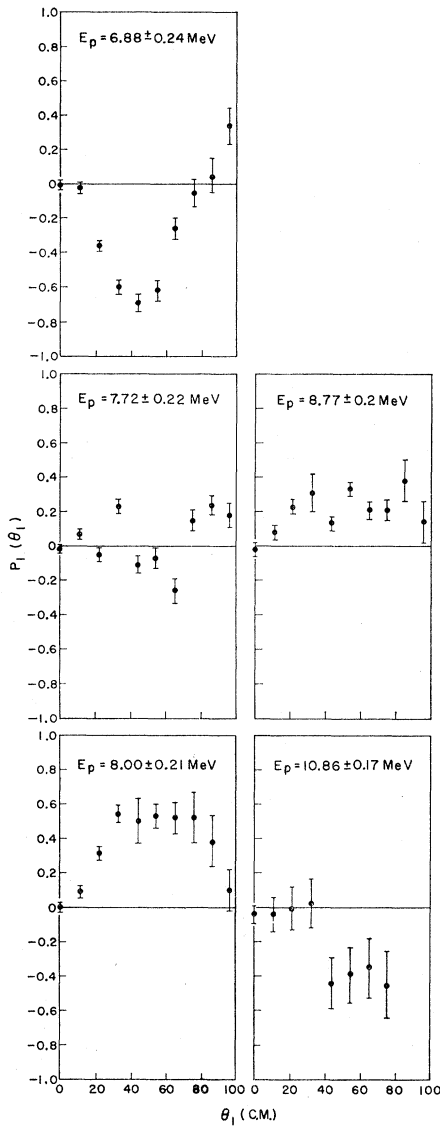


FIG. 5.  $P_1(\theta_1)$  for the  $C^{13}(p,n_0)N^{13}$  reaction.

function of the reaction angle  $\theta_1$ , the solenoid and shielding were mounted on a rotating platform fabricated from a 70-mm Army artillery unit and remotely controlled from the counting area.

A time-of-flight spectrum of the helium scattered neutrons for  $+\pi/2$  and  $-\pi/2$  precession is shown in Fig. 3. Two neutron peaks are seen corresponding to alternate proton bursts from the cyclotron (double display). The net number of "left" ( $+\pi/2$ ) and "right" ( $-\pi/2$ ) helium-scattered neutrons was found by summing over the two peaks and subtracting the corresponding background.

#### SOLENOID CALIBRATION

The solenoid magnet was calibrated by measuring the asymmetry  $R$  as a function of the solenoid current

for the  $C^{13}(p,n_0)N^{13}$  reaction at  $E_p=6.8$  MeV and  $\theta_1=40^\circ$ . The asymmetry should be a sinusoidal function of the solenoid current

$$R = P_1 P_2 \sin\left(\frac{\pi I}{2 I_0}\right), \quad (2)$$

where  $I_0$  is the current required for  $\pi/2$  precession. Assuming that the solenoid approximates an infinite solenoid,  $I_0$  (for  $E_n=3.6$  MeV) is calculated to be 325 A. Various values of  $R$  from Eq. (2) (with  $P_1 P_2 = -0.35$  and  $I_0=325$  A) along with the experimentally measured asymmetry are plotted in Fig. 4. The good agreement indicates that the solenoid field is well described by the infinite-solenoid equation.

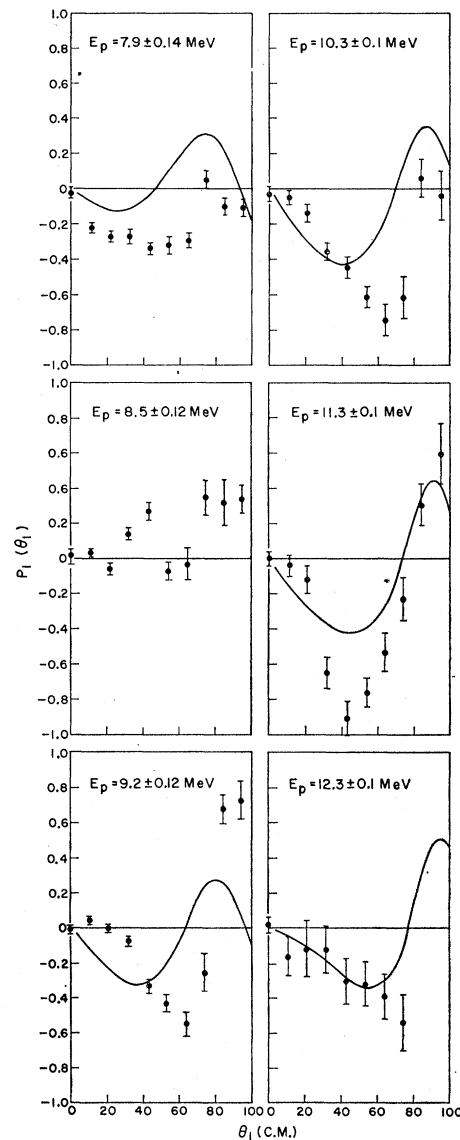


FIG. 6.  $P_1(\theta_1)$  for the  $N^{15}(p,n_0)O^{15}$  reaction. The solid curves are the polarization predictions obtained from the DWBA calculations.

## CHECKS ON SYSTEMATIC ERRORS

To check the effect of the magnetic fringe field of the solenoid on the photomultiplier gain, a gamma source ( $\text{Na}^{22}$ ) was placed next to the detector and the counting rate was observed for fields up to twice that used in the polarization measurements. The result indicated that within statistics the magnetic field did not effect the detector efficiency. Additionally, the presence of other possible sources of false asymmetries was investigated by measuring the asymmetry at  $\theta_1=0^\circ$ . At this angle there is no preferred direction for the vector  $\mathbf{P}_1$  and hence the polarization must vanish. This check was made before and after each polarization angular distribution measurement. Within statistics a null value for  $P_1$  was consistently obtained indicating the absence of false asymmetries.

Further, the angular dependence of the neutron polarizations was measured in two sets of  $20^\circ$  steps. That is, the order taken for  $\theta_1$  was 0, 20, 40, 60, and  $80^\circ$  followed by 90, 70, 50, 30, 10, and another  $0^\circ$ . Since the polarizations were expected to be smooth functions of the reaction angle, the fact that the values from the two sets indicated the same angular dependence (sign and magnitude) served as a measure of the long-term stability of the electronic and associated equipment.

## MULTIPLE SCATTERING CORRECTIONS

The unpolarized angular distributions<sup>14</sup> for neutrons scattered by helium were used to calculate single ( $p_1$ ), double ( $p_2$ ), and triple ( $p_3$ ) scattering probabilities as a function of the scattered neutron energy using a Monte Carlo code on the IBM 7094. Higher order events were negligible ( $<0.1\%$  probability). The variation of detector efficiency with neutron energy was also taken into account. The multiple scattering corrections were made by multiplying the measured asymmetry given by Eq. (1) by  $\sum_i^3 p_i'/p_i$ , where  $p_i'$  is the scattering probability modified by the detector efficiency. This method corrects the denominator of Eq. (1) exactly but makes the assumption that second and higher order events cancel by pairs in the numerator. This method of correction tends to overestimate the polarization magnitudes since second and higher order scattering events generally have the same polarization as for single scattering. The reason for this is that double scattering into the forward direction ( $\theta_2=60^\circ$ ) is more probable by two forward single scatterings thus retaining the sign of the polarization.<sup>15</sup> The multiple scattering corrections varied from 10 to 13%.

## RESULTS

The neutron polarizations  $P_1(\theta_1)$  were determined using Eq. (1) and are shown plotted in the center-of-

<sup>14</sup> M. D. Goldberg, V. M. May, and J. R. Stehn, BNL Report 400, 2nd ed., 1962, Vol. I (unpublished).

<sup>15</sup> For a full discussion, see A. J. Elwyn and R. O. Lane, Nucl. Phys. **31**, 78 (1962).

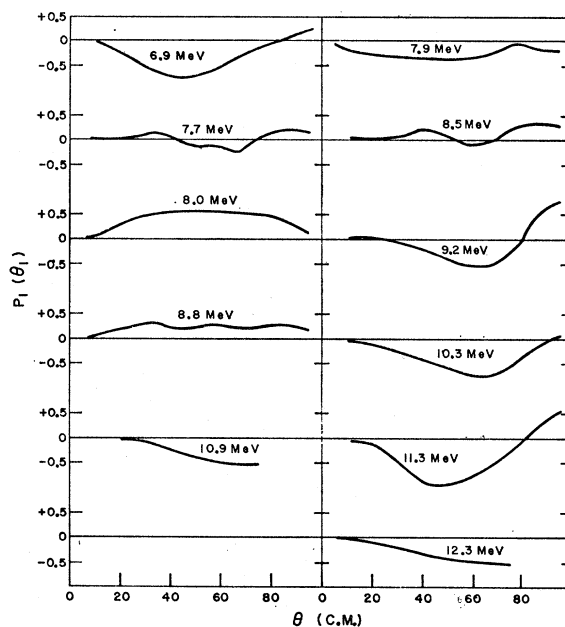
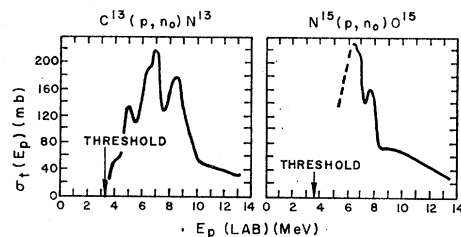


FIG. 7. Comparison of  $\sigma_t(E_p)$  with  $P_1(\theta_1, E_p)$  for the  $\text{C}^{13}(p, n_0)\text{N}^{13}$  and  $\text{N}^{15}(p, n_0)\text{O}^{15}$  reactions.

mass system in Figs. 5 and 6. Multiple scattering corrections have been applied. The values used for  $P_2(60^\circ)$  were computed<sup>16</sup> from Seagrave's<sup>17</sup>  $n$ - $\alpha$  phase shifts. Measurements of the analyzing power of helium by May *et al.*,<sup>18</sup> are in good agreement with values calculated from these phase shifts over the energy region of interest in this experiment. The errors shown on the magnitudes of  $P_1$  are computed only from statistical counting errors on the asymmetry  $P_1P_2$ . The proton beam energy spreads indicated are due to the beam energy loss in the gas targets.

## DISCUSSION

Figure 7 displays both  $\sigma_t(E_p)$  and  $P_1(\theta_1, E_p)$  for the two  $(p, n_0)$  reactions. The total  $(p, n_0)$  cross-section measurements are those of Wong *et al.*,<sup>1</sup> and smooth curves have been drawn through both these and the polarization data. Here it is observed that for both reactions the rapid fluctuation of  $P_1$  with proton energy is well correlated with the pronounced resonance struc-

<sup>16</sup> L. Stewart (private communication).

<sup>17</sup> J. D. Seagrave, Phys. Rev. **92**, 1222 (1953).

<sup>18</sup> T. H. May, R. L. Walter, and H. H. Barschall, Nucl. Phys. **45**, 17 (1963).

ture of  $\sigma_i$ . Specifically for  $C^{13}+p$ , the neutron polarizations (for  $\theta_1 < 90^\circ$ ) change from generally negative (6.9 MeV) to positive (8.0 and 8.8 MeV) and again to negative (10.9 MeV) values as the total cross section goes through various maxima and minima.

Whereas the angular distributions for these two reactions are similar (see Ref. 1), thus supporting the twin direct reaction concept as hypothesized by Bloom *et al.*,<sup>2</sup> the neutron polarizations only approach semblance at the highest energies measured. Since differential cross sections are less sensitive to the details of the interaction than are neutron polarizations, it is not surprising that the simple direct interaction model of Bloom *et al.*<sup>2</sup> finds support in the measurements of Wong *et al.*<sup>1</sup> and not in the results shown here. However, it is interesting to compare the polarization energy dependence of the two reactions. Figure 8 is a comparison of  $P_1(E_q)$  for the two reactions at  $\theta_1 = 30, 50, 70,$  and  $90^\circ$  (lab). By using equivalent energies defined as  $E_q = (A/A+1)E_p - (1/2)Q$ , an attempt is made to reduce effects due to the  $Q$ -value difference between these reactions (see Ref. 1). Although a detailed interpretation must await the results of calculations now in progress,<sup>19</sup> the apparent correspondence of the energy dependence between the two reactions in the forward angles can hardly be regarded as fortuitous.

The solid curves (Fig. 6) represent the polarization predictions obtained by considering the  $N^{15}(p,n_0)O^{15}$  reaction as a quasielastic process in DWBA.<sup>20</sup> The parameters chosen for these calculations were those that were used to generate the  $N^{15}(p,n_0)O^{15}$  angular distributions,<sup>9</sup> i.e.,  $r_0 = 1.25$  F,  $a = 0.65$  F,  $a' = 0.47$  F,  $W = 8$  MeV,  $V_{so} = 6$  MeV, and  $V = 46$  MeV for neutrons and 51 MeV for protons. (The notation is that of Ref. 9.) The strength of the isospin potential  $V_1$  was adjusted to fit the angular distributions, but in DWBA the neutron polarizations are independent of  $V_1$ . No polarization predictions are available for the  $C^{13}(p,n_0)N^{13}$  reaction.

The polarization predictions generated by the DWBA calculations are only in fair agreement with experiment. The general features of the measurements are reproduced however, and the agreement does improve above the resonance region. The discrepancies could result from at least two factors: (1)  $N^{15}$  is perhaps too light to be described by an optical model, and (2) these calculations neglect particle-hole interactions which are known to be quite strong<sup>21</sup> for  $O^{16}$  ( $N^{15}$  is well approximated by an  $O^{16}$  core with a  $p_{1/2}$  proton hole).

<sup>19</sup> S. D. Bloom (private communication).

<sup>20</sup> We are indebted to G. R. Satchler for these calculations.

<sup>21</sup> R. H. Lemmer, Phys. Letters 4, 205 (1963).

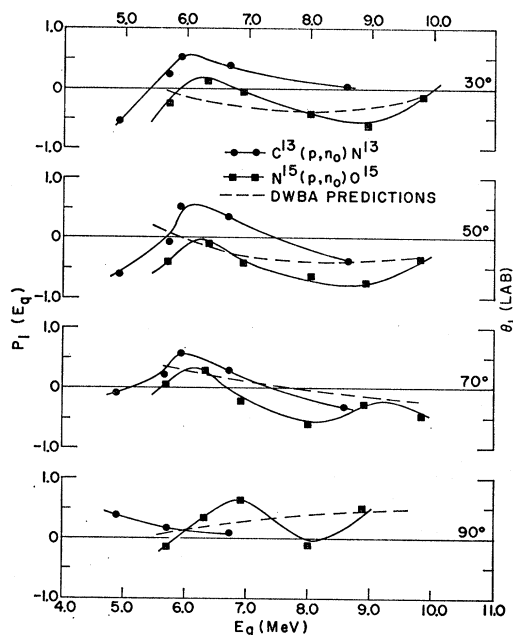


FIG. 8. Comparison of  $P_1(E_q)$  for the  $C^{13}(p,n_0)N^{13}$  and  $N^{15}(p,n_0)O^{15}$  reactions with DWBA predictions.

Figure 8 also displays the quasielastic predictions which yield essentially horizontal curves, i.e., polarizations resulting from a spin-orbit potential are not strongly energy-dependent. The observed deviations from such curves could thus be inferred as arising from the spin dependence of the neglected particle-hole interactions, with the net (measured) polarizations thus resulting from the "sum" of the two effects.

Finally, the measurements indicate that these two reactions are quite useful as sources of polarized neutrons in this energy region. In particular, for  $E_p = 6.9$  MeV and  $\theta_1 = 40^\circ$  lab, the  $C^{13}(p,n_0)N^{13}$  reaction produces 3.7-MeV neutrons with appreciable polarizations ( $P_1 = -0.70 \pm 0.04$ ). The differential cross section for this case is also large ( $d\sigma/d\Omega = 22.6 \pm 0.6$  mb/sr<sup>1</sup>).

#### ACKNOWLEDGMENTS

The continued interest and support of Dr. H. Mark is sincerely appreciated. Special mention should also be made of the various support groups associated with this work. In particular, the competent engineering of Harold Brooks and Frank Dodd, the technical assistance of Lee Talbot, and the cooperation of the cyclotron crew under Donald Rawles is gratefully acknowledged. Last, but not least, special thanks is given to Don Davis and Bill Rice for programming the Monte Carlo calculations on the IBM 7094.